



# CHORUS

This is the accepted manuscript made available via CHORUS. The article has been published as:

## Neutron Single Particle Structure in $^{131}\text{Sn}$ and Direct Neutron Capture Cross Sections

R. L. Kozub, G. Arbanas, A. S. Adekola, D. W. Bardayan, J. C. Blackmon, K. Y. Chae, K. A. Chipps, J. A. Cizewski, L. Erikson, R. Hatarik, W. R. Hix, K. L. Jones, W. Krolas, J. F. Liang, Z. Ma, C. Matei, B. H. Moazen, C. D. Nesaraja, S. D. Pain, D. Shapira, J. F. Shriner, Jr., M. S. Smith, and T. P. Swan

Phys. Rev. Lett. **109**, 172501 — Published 24 October 2012

DOI: [10.1103/PhysRevLett.109.172501](https://doi.org/10.1103/PhysRevLett.109.172501)

# Neutron single particle structure in $^{131}\text{Sn}$ and direct neutron capture cross sections

R. L. Kozub,<sup>1</sup> G. Arbanas,<sup>2</sup> A. S. Adekola,<sup>3,4</sup> D. W. Bardayan,<sup>5</sup> J. C. Blackmon,<sup>5,\*</sup> K.Y. Chae,<sup>6,7</sup> K. A. Chipps,<sup>8</sup> J. A. Cizewski,<sup>4</sup> L. Erikson,<sup>8,†</sup> R. Hatarik,<sup>4,‡</sup> W. R. Hix,<sup>5,6</sup> K. L. Jones,<sup>6</sup> W. Krolas,<sup>9</sup> J. F. Liang,<sup>5</sup> Z. Ma,<sup>6</sup> C. Matei,<sup>10,§</sup> B. H. Moazen,<sup>6</sup> C. D. Nesaraja,<sup>5</sup> S. D. Pain,<sup>4,5</sup> D. Shapira,<sup>5</sup> J. F. Shriner, Jr.,<sup>1</sup> M. S. Smith,<sup>5</sup> and T. P. Swan<sup>4,11</sup>

<sup>1</sup>*Department of Physics, Tennessee Technological University, Cookeville, TN 38505, USA*

<sup>2</sup>*Reactor and Nuclear Systems Division, Oak Ridge National Laboratory, Oak Ridge, TN 37831-6171 USA*

<sup>3</sup>*Department of Physics and Astronomy, Ohio University, Athens, OH 45701 USA*

<sup>4</sup>*Department of Physics and Astronomy, Rutgers University, Piscataway, NJ 08854-8019 USA*

<sup>5</sup>*Physics Division, Oak Ridge National Laboratory, Oak Ridge, TN 37831 USA*

<sup>6</sup>*Department of Physics and Astronomy, University of Tennessee, Knoxville, TN 37996 USA*

<sup>7</sup>*Department of Physics, Sungkyunkwan University, Suwon 440-746, Korea*

<sup>8</sup>*Department of Physics, Colorado School of Mines, Golden, CO 80401 USA*

<sup>9</sup>*Institute of Nuclear Physics, PAN, Krakow, Poland*

<sup>10</sup>*Oak Ridge Associated Universities, Bldg 6008, P. O. Box 2008, Oak Ridge, TN 37831-6374 USA*

<sup>11</sup>*Department of Physics, University of Surrey, Guilford, Surrey, GU2 7XH, UK*

(Dated: September 14, 2012)

Recent calculations suggest that the rate of neutron capture by  $^{130}\text{Sn}$  has a significant impact on late-time nucleosynthesis in the r-process. Direct capture into low-lying bound states is expected to be significant in neutron capture near the  $N=82$  closed shell, so r-process reaction rates may be strongly impacted by the properties of neutron single particle states in this region. In order to investigate these properties, the  $(d,p)$  reaction has been studied in inverse kinematics using a 630 MeV beam of  $^{130}\text{Sn}$  (4.8 MeV/u) and a  $(\text{CD}_2)_n$  target. An array of Si strip detectors, including the SIDAR and an early implementation of the ORRUBA, was used to detect reaction products. Results for the  $^{130}\text{Sn}(d,p)^{131}\text{Sn}$  reaction are found to be very similar to those from the previously reported  $^{132}\text{Sn}(d,p)^{133}\text{Sn}$  reaction. Direct-semidirect  $(n,\gamma)$  cross section calculations, based for the first time on experimental data, are presented. The uncertainties in these cross sections are thus reduced by orders of magnitude from previous estimates.

PACS numbers: 21.10.Jx, 25.45.Hi, 25.60.Je, 26.30.Hj, 25.40.Lw, 29.38Gj

Keywords:

The rapid neutron capture process (r-process) is thought to be responsible for the synthesis of about half of the nuclear species heavier than Fe [1], but little experimental nuclear physics information is available for r-process studies. Recent r-process calculations by Beun *et al.* [2] and Surman *et al.* [3] suggest the  $^{130}\text{Sn}(n,\gamma)^{131}\text{Sn}$  reaction rate plays a pivotal role in nucleosynthesis, engendering global effects on isotopic abundances over a wide mass range during the freeze-out epoch following  $(n,\gamma)\rightleftharpoons(\gamma,n)$  equilibrium. This is owing, in part, to the long  $\beta$ -decay lifetime of the  $^{130}\text{Sn}$  ground state (322 s). Direct neutron capture (DC) is expected to be significant at late times in the r-process near the  $N=82$  closed shell, and the reaction rate may thus be strongly impacted by the properties of single particle states in this region. The most critical states for s-wave DC are the  $3p_{3/2}$  and  $3p_{1/2}$  single neutron states, which would be populated via E1 transitions. The DC cross section varies widely depending on whether or not these states are bound [4], and their excitation energies were not known before the present work. Indeed, theoretical DC  $(n,\gamma)$  cross sections can vary by nearly three orders of magnitude for  $^{130}\text{Sn}$ , depending on the nuclear structure model selected [4]. Thus, neutron single-particle data on neutron-rich

species in this region are crucial for evaluating the role of  $^{130}\text{Sn}$  in the r-process and for constraining model parameters.

Yrast cascades in  $^{131}\text{Sn}$  involving states with  $J\geq 11/2$  have been studied by Bhattacharyya *et al.* [5], and the spins and parities of some of the low-lying hole states have been assigned tentatively from  $\beta$ -decay experiments [6],[7]. Since there are nominally two neutron holes in the  $^{130}\text{Sn}$  core ( $N=80$ ), one or more low-lying, low angular momentum hole states of  $^{131}\text{Sn}$  may be observed in a  $(d,p)$  experiment, depending on the complexity of the  $^{130}\text{Sn}$  ground state wave function. From shell model considerations, the highest orbitals below the  $N=82$  shell gap are expected to be the (nearly degenerate)  $2d_{3/2}$  and  $1h_{11/2}$ , plus the  $3s_{1/2}$ . From the recent  $^{132}\text{Sn}(d,p)^{133}\text{Sn}$  work of Jones *et al.* [8], the lowest orbital above the  $N=82$  gap is expected to be the  $2f_{7/2}$ , followed by (in order)  $3p_{3/2}$ ,  $3p_{1/2}$ ,  $1h_{9/2}$ , and  $2f_{5/2}$ , all of which are vacant in  $^{130}\text{Sn}$ . Since  $\ell=5$  transfers are very weak in the  $(d,p)$  reaction at the energy used here (4.8 MeV/u), one expects the strongest states to be  $\ell=1$  and  $\ell=3$  transfers coupled to the  $^{130}\text{Sn}$  ground state, i. e., negative-parity  $1p$ - $2h$  states. No single-particle information for any of these states in  $^{131}\text{Sn}$  has been reported from previous

measurements. As mentioned above, the  $\ell=1$ ,  $3p_{3/2}$  and  $3p_{1/2}$  single-neutron states are of particular importance for DC in the r-process, as this typically involves the capture of an s-wave neutron followed by an E1  $\gamma$ -ray transition. In this paper, results from the first experiment to investigate directly the single-particle properties of states in  $^{131}\text{Sn}$  are reported and direct-semidirect ( $n, \gamma$ ) cross section calculations based on those data are presented.

The experimental technique has been described earlier [9], and is essentially identical to that used for the ( $d, p$ ) study of doubly magic  $^{132}\text{Sn}$  [8]. A radioactive beam of 630-MeV  $^{130}\text{Sn}$  ions (4.8 MeV/u), accelerated at the Holifield Radioactive Ion Beam Facility (HRIBF) at Oak Ridge National Laboratory (ORNL), bombarded an 80  $\mu\text{g}/\text{cm}^2$ -thick  $(\text{CD}_2)_n$  foil. In order to detect protons near  $90^\circ$  in the laboratory, the target surface was placed at  $30^\circ$  with respect to the beam axis, so the effective areal density was  $\simeq 160 \mu\text{g}/\text{cm}^2$ . The beam intensity was  $\sim 2 \times 10^5$  ions/s. Reaction products were detected with arrays of silicon strip detectors, including an early implementation of the Oak Ridge Rutgers University Barrel Array (ORRUBA) [10] and the ORNL Silicon Detector Array (SIDAR) [11]. (The SIDAR was mounted at large laboratory angles (small center-of-mass angles) to detect protons from possible  $\ell=0$  transitions, but no evidence for such transitions was observed.) The ORRUBA consisted of ten 1000- $\mu\text{m}$ -thick position sensitive silicon strip detectors, plus four thinner  $\Delta E$  detectors that were used to form detector telescopes for the more forward angles. Mounted downstream from these arrays were (in order) an annular silicon strip detector, a carbon-foil-microchannel plate detector (MCP), and a segmented-anode ion counter. These detectors were used for beam diagnostics. Coincidence signals from particles detected in the silicon arrays and the beam-like recoils striking the MCP served to reduce the background from other, non- $(d, p)$  processes. Proton loci from the inverse  $(d, p)$  reaction were identified in the energy- versus-angle event spectra by comparison to calculated kinematics lines. Cross section normalization was achieved by detecting elastically scattered deuterons with the ORRUBA at relatively small center-of-mass angles ( $33^\circ$ - $38^\circ$ ), where the ratio to Rutherford scattering is in the range 0.92-0.99, and comparing to optical model calculations. The estimated uncertainty in normalization is 10%. Corrections for energy loss in the target were made for both the beam and the emitted protons. Excitation energies in  $^{131}\text{Sn}$  were deduced using as a calibration known states excited via the  $^2\text{H}(^{132}\text{Sn}, p)^{133}\text{Sn}$  reaction [8] with the same detectors and target. This worked quite well, as the ranges of reaction Q-values overlap nicely for the two experiments. However, the absence of clear evidence for any previously known levels in  $^{131}\text{Sn}$  necessitated the inclusion of uncertainties in the masses of all the isotopes involved in the calibration ( $^{130}$ - $^{133}\text{Sn}$ ) in determining the errors for the  $^{131}\text{Sn}$  excitation energies. This contribution

is about 30 keV [12],[13] and we estimate an excitation energy uncertainty of  $\pm 50$  keV.

A Q-value spectrum from a forward-angle strip detector is shown in Fig. 1. This spectrum is remarkably similar to that acquired in the ( $d, p$ ) reaction study on doubly magic  $^{132}\text{Sn}$  [8], in which the lowest strong state was the  $^{133}\text{Sn}$  ground state, which has most of the  $2f_{7/2}$  single particle strength. In both experiments, four strong proton groups are observed, presumably corresponding to single-particle  $2f_{7/2}$ ,  $3p_{3/2}$ ,  $3p_{1/2}$ , and  $2f_{5/2}$  states, and the level spacings are about the same in the two residual nuclei (Fig. 2). The excitation energy range is  $\sim 2.6$ - $4.7$  MeV in  $^{131}\text{Sn}$ . Prior to the present work, none of these levels had been reported. It is interesting to note that the lowest strong state in  $^{131}\text{Sn}$  is close to where the  $2f_{7/2}$  single particle state is expected ( $\sim 2.8$  MeV), based on a simple weak coupling calculation [14]. The angular distribution data (Fig. 3) indicate the level at 2.6 MeV is indeed consistent with an  $\ell=3$  angular momentum transfer. Further, the angular distributions for the 3.4- and 4.0-MeV groups are both consistent with  $\ell=1$  transfers, suggesting the order of single particle levels is probably similar to that in  $^{133}\text{Sn}$ . On this basis, the 4.7-MeV group is tentatively assigned ( $5/2^-$ ), even though the angular distribution is not sufficiently definitive to rule out other possibilities. The dotted curves in Fig. 3 are  $2f_{7/2}$  and  $2f_{5/2}$  calculations for the 3404- and 3986-keV levels, respectively (both with  $S=1.00$ ), to illustrate the strong preference at small angles for  $\ell=1$  assignments for these states. The experimental results for  $^{131}\text{Sn}$  are summarized in Table I. The spectroscopic factors listed in Table I can be compared directly to the DWBA spectroscopic factors for  $^{133}\text{Sn}$  [8], as they were obtained using the same bound state potential parameters and the same source of optical model parameters [15].

It should be noted that a similar correspondence of single particle strength between  $^{207}\text{Pb}$  and  $^{209}\text{Pb}$  was observed by Mukherjee and Cohen [18], who studied the ( $d, p$ ) reaction on  $^{206}\text{Pb}$  and doubly magic  $^{208}\text{Pb}$ . Even though a similar pattern was observed in the  $^{206}\text{Pb}(d, p)^{207}\text{Pb}$  spectra of these authors, the apparent concentration of fp-shell single particle strength in only one main level for each orbital in  $^{131}\text{Sn}$  is somewhat surprising, given that  $^{130}\text{Sn}$  is only semi-magic. This relative lack of fragmentation suggests that the  $Z=50$  proton core is intact, and that the  $^{130}\text{Sn}$  ground state has a simple neutron structure as well. In contrast, the semi-magic nucleus  $^{134}\text{Te}$  ( $Z=52$ ,  $N=82$ ) is apparently not so simple, as the neutron single-particle strength in  $^{135}\text{Te}$  was found to be significantly fragmented in a ( $d, p$ ) study, also performed at the HRIBF [19].

The  $^{131}\text{Sn}$  ground state is believed to be  $3/2^+$ , with the first excited state being the  $1h_{11/2}$  hole state at about 65 keV excitation [20]. Neither of these states was observed in the present experiment. If the two neutron holes in

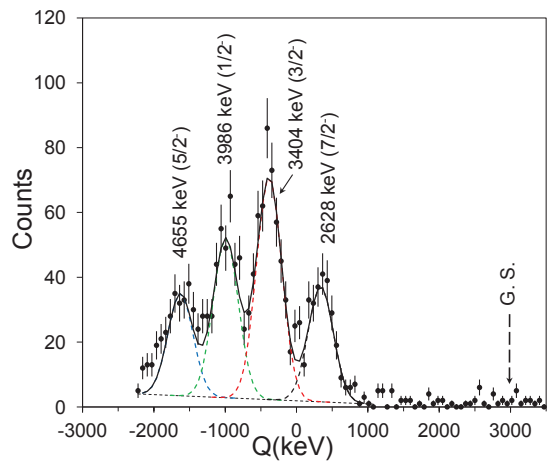


FIG. 1: (Color online) Q-value spectrum of protons from a forward-angle strip detector of the ORRUBA, covering laboratory angles between about  $69^\circ$  and  $90^\circ$ . Approximate  $^{131}\text{Sn}$  excitation energies, assumed spins and parities, and nominal position of the unobserved ground state are also shown. The strong peak region is fitted with four Gaussians of equal width, for which the  $\chi^2$  per degree of freedom is 1.46. The background in the low Q-value region (low proton energies) is owing mostly to setting analysis thresholds close to detector noise levels.

TABLE I: Properties of single particle states in  $^{131}\text{Sn}$  from the inverse  $^{130}\text{Sn}(d,p)^{131}\text{Sn}$  reaction. Estimated uncertainties in spectroscopic factors ( $S$ ) are primarily owing to ambiguities in the direct reaction model.

$E_x(\text{keV})$ ( $\pm 50$ keV)	$J^\pi$	$S$ ( $\pm 30\%$ )
2628	$(7/2^-)$	0.70
3404	$(3/2^-)$	0.70
3986	$(1/2^-)$	1.00
4655	$(5/2^-)$	0.75

the  $^{130}\text{Sn}$  ground state were in the  $2d_{3/2}$  orbital, the orbital would be half-empty and the spectroscopic factor  $S$  could be as large as 0.5. An upper limit of 0.3 is consistent with the data from the present experiment. Of course, from shell and pairing model considerations [21, 22], the ground state wave function of  $^{130}\text{Sn}$  is expected to be a linear combination of hole pairs in the  $1h_{11/2}$ ,  $2d_{3/2}$ ,  $3s_{1/2}$ ,  $2d_{5/2}$ , and  $1g_{7/2}$  orbitals, roughly in order of decreasing coefficients [14]. This suggests there is a significant probability that the two neutron holes in  $^{130}\text{Sn}$  are in the  $1h_{11/2}$  orbital, as it is nearly degenerate with the  $2d_{3/2}$  [20], and  $\ell=5$  transfers would be very weak in the  $(d,p)$  reaction at our beam energy (4.8 MeV/u). Indeed, even with the hole pair only in the  $1h_{11/2}$  orbital ( $S=0.17$ ), the maximum differential cross section for  $\ell=5$  would be  $\sim 0.1$  mb/sr, a factor of 20 lower than the smallest measured in the present experiment. Also, from a purely statistical point of view, it is three times more likely for the holes to lie in the  $1h_{11/2}$  than in the

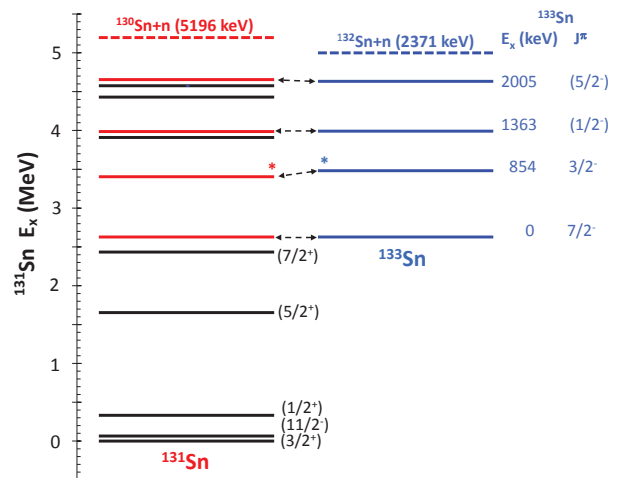


FIG. 2: (Color online) Energy levels observed in the  $(d,p)$  reaction on  $^{130}\text{Sn}$  (in red on left) and  $^{132}\text{Sn}$  (right) [8]. The energy corresponding to the  $^{133}\text{Sn}$  ground state has been shifted to align with the lowest state observed in  $^{131}\text{Sn}$ . (For a Q-value comparison, the energy levels of  $^{133}\text{Sn}$  should be shifted upward by 197 keV, so neutron thresholds are aligned.) The states flagged with an asterisk (\*) were the strongest in the respective experiments. Lower known states in  $^{131}\text{Sn}$  [6] are also shown, but they were not observed in the present work.

$2d_{3/2}$  orbital.

As mentioned earlier, the observation of  $\ell=1$  strength in  $^{131}\text{Sn}$  is important for direct neutron capture and its potential impact on r-process nucleosynthesis. There is also a semi-direct capture via the giant dipole resonance (GDR), which is accounted for by adding a GDR term to the single-particle electromagnetic operator. Direct-semidirect (DSD) neutron capture cross sections for  $^{130}\text{Sn}$  were calculated using the data in Table I and the code CUPIDO [23]. For low energy capture, the code implements a conventional potential model expressed in terms of single-particle electromagnetic transition matrix elements computed in a first-order approximation. In the incident channel the real part of a phenomenological Koning-Delaroche potential [24] was used. The imaginary part of these potentials is dropped because the loss of flux into other channels is expected to be small [25]. For the bound-state single-neutron wave functions the Bear-Hodgson potential [26] was used, where the depth was fitted to reproduce binding energies for each of the capturing bound states in Table I. The DSD capture cross sections are plotted in Figure 4 between 0.01 and 6 MeV for computation of Maxwellian averages at astrophysical temperatures. At 30 keV the total computed DSD cross section is 0.14 mb for the real parts of the Koning-Delaroche potential with an uncertainty of  $\approx 20\%$ . A slight variance with a DSD capture computation of  $\approx 0.22$  mb reported by Chiba *et al.* [27] is likely due to using different single-particle level energies or a

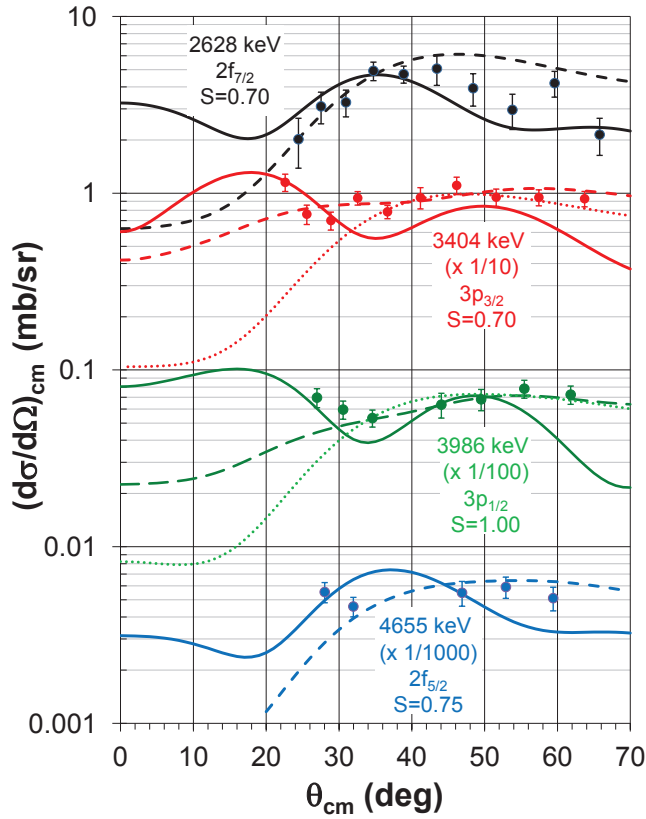


FIG. 3: (Color online) Angular distributions of protons from ORRUBA detectors, extracted using bins of  $5^\circ$  angular width in the laboratory. The 3986- and 4655-keV distributions have fewer points, owing to low proton energies being below detector thresholds at some angles. Dashed curves are distorted wave Born approximation (DWBA) calculations using the optical parameters of Strömich *et al.* [15] and the solid curves are the same calculations except for using the “BG” parameters of Sen *et al.* [16] in the proton channel (obtained by fitting  $^{136}\text{Xe}(p,p)^{136}\text{Xe}$  elastic scattering data). The “standard” bound state parameters of  $r_0=1.25$  fm and  $a=0.65$  fm were used for all cases. For each level, the dashed and solid curves are shown for the same spectroscopic factor. Dotted curves are  $2f_{7/2}$  and  $2f_{5/2}$  calculations for the 3404- and 3986-keV levels, respectively (both with  $S=1.00$ ), to illustrate the strong preference at small angles for  $\ell=1$  assignments for these states. The exact finite range code DWUCK5 [17] was used for the calculations. See text for discussion of tentative  $J^\pi$  assignments.

different single-particle bound-state potential [28].

Reaction rate and nucleosynthesis calculations require  $(n, \gamma)$  cross sections for both DSD capture and statistical capture. The latter depend heavily on the level density in the Gamow window, and while that is not yet well established for  $^{131}\text{Sn}$ , there are reasons to believe that the level density so close to the  $N=82$  closed shell is too low for statistical capture to dominate. In any case, the results of the present work will be an absolutely necessary ingredient for reaction rate calculations that may be done in the future, and are thus a critical component for de-

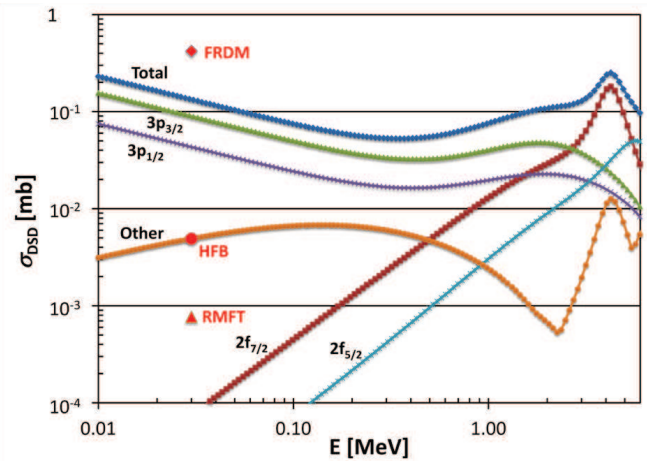


FIG. 4: (Color online) Direct-semidirect capture cross sections for the  $^{130}\text{Sn}(n, \gamma)^{131}\text{Sn}$  reaction computed using the code CUPIDO [23] for real parts of a phenomenological Koning-Delaroche [24] optical model potential are plotted for levels in Table I. An upper limit for the combined DSD capture into the  $1h_{11/2}$ ,  $2d_{3/2}$ ,  $3s_{1/2}$ ,  $2d_{5/2}$ , and  $1g_{7/2}$  orbitals (labeled “other”) is not included in the total DSD. Shown for comparison (single red points) are the calculations of Rauscher *et al.* [4] for 30 keV neutrons using the Finite Range Droplet (FRDM), the Hartree-Fock-Bogoliubov (HFB), and Relativistic Mean Field Theory (RMFT) models. Of these, only the FRDM predicted both the  $3p_{3/2}$  and  $3p_{1/2}$  single-neutron states to be bound.

termining the impact of the important  $^{130}\text{Sn}(n, \gamma)^{131}\text{Sn}$  reaction on global isotopic abundances in the r-process.

In summary, the inverse  $^{130}\text{Sn}(d, p)^{131}\text{Sn}$  reaction has been investigated at 4.8 MeV/u. An apparent single-particle spectrum is observed, very similar to that observed in the  $(d, p)$  reaction on doubly magic  $^{132}\text{Sn}$ . Measurements have been made of excitation energies and angular distributions, and  $\ell$  assignments are consistent with expected single particle states. In particular, the presumed  $\ell=1$  single particle states are both bound, which favors a relatively large DC cross section compared to those from models that predict one or both of these states to be unbound [4]. Using these experimental results, cross sections for  $^{130}\text{Sn}(n, \gamma)^{131}\text{Sn}$  direct-semidirect capture have been calculated, and, for reasons stated earlier, the uncertainties are reduced by orders of magnitude from previous estimates, none of which was based on experimental data. This information will also help to constrain nuclear models and facilitate more realistic  $(n, \gamma)$  reaction rate calculations for r-process nucleosynthesis involving other isotopes. At present, we defer calculation of the  $^{130}\text{Sn}(n, \gamma)^{131}\text{Sn}$  reaction rate and r-process nucleosynthesis, as contributions from statistical processes are not well understood at this time.

This work was supported by the U. S. Department of Energy under contract numbers DE-FG02-96ER40955 (TTU), DE-FG52-03NA00143 (Rutgers,

ORAU), DE-AC05-00OR22725 (ORNL), DE-FG02-96ER40990 (TTU), DE-FG03-93ER40789 (Mines), DE-FG02-96ER40983 (UTK), DE-SC0001174 (UTK), and the National Science Foundation under contract number NSF-PHY-00-098800 (Rutgers). Computation of direct-semidirect capture was supported by Topical Collaboration on Theory for Reactions on Unstable iSotopes (TORUS: [www.reactiontheory.org](http://www.reactiontheory.org)). The authors also acknowledge useful discussions with R. Surman, J. Beun, and B. A. Brown.

- 
- \* Current address Department of Physics and Astronomy, Louisiana State University, Baton Rouge, LA 70803 USA
- † Current address Pacific Northwest National Laboratory, P.O. Box 999, Richland, Washington 99352, USA
- ‡ Current address Lawrence Livermore National Laboratory, Livermore, CA 94550 USA
- § Current address European Commission-Joint Research Centre, Institute for Reference Materials and Measurements, Retieseweg 111 2440 GEEL, Belgium
- [1] E. M. Burbidge *et al.*, *Rev. Mod. Phys.* **29**, 547 (1957).
- [2] J. Beun *et al.*, *J. Phys. G: Nucl. Part. Phys.* **36**, 025201 (2009).
- [3] R. Surman, J. Beun, G. C. McLaughlin, and W. R. Hix, *Phys. Rev. C* **79**, 045809 (2009).
- [4] T. A. Rauscher *et al.*, *Phys. Rev. C* **57**, 2031 (1998).
- [5] P. Bhattacharyya *et al.*, *Phys. Rev. Lett.* **87**, 062502 (2001).
- [6] Yu. Khazov, I. Mitropolsky, A. Rodionov, *Nuclear Data Sheets* **107**, 2715 (2006).
- [7] <http://www.nndc.bnl.gov/chart/getdataset.jsp?nucleus=131SN&unc=nds> (2012).
- [8] K. L. Jones *et al.*, *Nature* **465**, 454 (2010); *Phys. Rev. C* **84**, 034601 (2011).
- [9] R. L. Kozub *et al.*, 10th Symposium on Nuclei in the Cosmos, *Proceedings of Science*, **PoS(NIC X)**, 135 (2008).
- [10] S. D. Pain *et al.*, *Nucl. Instr. Meth.* **B261**, 1122 (2007).
- [11] D. W. Bardayan *et al.*, *Phys. Rev. Lett.* **83**, 45 (1999).
- [12] M. Dworschak *et al.*, *Phys. Rev. Lett.* **100**, 072501 (2008).
- [13] G. Audi *et al.*, *Nucl. Phys.* **A729**, 337 (2003).
- [14] B. A. Brown, private communication (2008).
- [15] A. Strömich *et al.*, *Phys. Rev. C* **16** 2193 (1977).
- [16] S. Sen, P. J. Riley, and T. Udagawa, *Phys. Rev. C* **6**, 2201 (1972).
- [17] P. D. Kunz, <http://spot.colorado.edu/~kunz/DWBA.html>, unpublished.
- [18] Paresh Mukherjee and Bernard L. Cohen, *Phys. Rev.* **127**, 1284 (1962).
- [19] S. D. Pain *et al.*, 10th Symposium on Nuclei in the Cosmos, *Proceedings of Science*, **PoS(NIC X)**, 142 (2008).
- [20] B. Fogelberg *et al.*, *Phys. Rev. C* **70** 034312 (2004).
- [21] V. G. Zelevinsky and A. Volya, *Phys. At. Nucl.* **66**, 1781 (2003).
- [22] R. W. Richardson and N. Sherman, *Nucl. Phys.* **52**, 221 (1964); **52**, 253 (1964).
- [23] W. E. Parker *et al.*, *Phys. Rev. C* **52**, 252 (1995).
- [24] A. J. Koning and J. P. Delaroche, *Nucl. Phys. A* **713**, 231 (2003).
- [25] E. Kraussmann *et al.*, *Phys. Rev. C* **53**, 469 (1996).
- [26] K. Bear and P. E. Hodgson, *J. Phys. (London) G* **4**, L287 (1978).
- [27] S. Chiba *et al.*, *Phys. Rev. C* **77**, 015809 (2008).
- [28] H. Koura and M. Yamada, *Nucl. Phys. A* **671**, 96 (2000).